ESC HEART FAILURE
ESC Heart Failure (2020)
Published online in Wiley Online Library (wileyonlinelibrary.com) **DOI:** 10.1002/ehf2.12846

ORIGINAL RESEARCH ARTICLE

Assessment of diastolic dysfunction: comparison of different cardiovascular magnetic resonance techniques

Josephine Kermer[1], Julius Traber[1], Wolfgang Utz[1], Pierre Hennig[1], Marius Menza[2], Bernd Jung[3], Andreas Greiser[4], Philipp Barckow[5], Florian von Knobelsdorff-Brenkenhoff[1,6], Agnieszka Töpper[1,7], Edyta Blaszczyk[1,8] and Jeanette Schulz-Menger[1,8,9]*

[1]*Charité—Universitätsmedizin Berlin, corporate member of Freie Universität Berlin, Humboldt-Universität zu Berlin, and Berlin Institute of Health, Working Group on Cardiovascular Magnetic Resonance, Experimental and Clinical Research Center, a joint cooperation between the Charité Medical Faculty and the Max Delbrueck Center for Molecular Medicine, Lindenberger Weg 80, Berlin, 13125, Germany;* [2]*Department of Radiology, Medical Physics, Medical Center—University of Freiburg, Faculty of Medicine, University of Freiburg, Freiburg, Germany;* [3]*Institute of Diagnostic, Interventional and Paediatric Radiology, University Hospital Bern, Bern, Switzerland;* [4]*Siemens Healthineers GmbH, Erlangen, Germany;* [5]*Circle Cardiovascular Imaging Inc., Calgary, Alberta, Canada;* [6]*Department of Cardiology, Clinic Agatharied, Academic Teaching Hospital of the Ludwig-Maximilians-University of Munich, Munich, Germany;* [7]*Zentrum für Innere Medizin, Kardiologie, Angiologie und Notfallambulanz, Johanniter-Krankenhaus Genthin-Stendal, Akut- und Schwerpunktkrankenhaus, Akademisches Lehrkrankenhaus Otto-von-Guericke-Universität Magdeburg, Stendal, Germany;* [8]*DZHK (German Centre for Cardiovascular Research), partner site Berlin, Berlin, Germany;* [9]*Department of Cardiology and Nephrology, HELIOS-Kliniken Berlin-Buch, Schwanebecker Chaussee 50, Berlin, 13125, Germany*

Abstract

Aims Heart failure with preserved ejection fraction is still a diagnostic and therapeutic challenge, and accurate non-invasive diagnosis of left ventricular (LV) diastolic dysfunction (DD) remains difficult. The current study aimed at identifying the most informative cardiovascular magnetic resonance (CMR) parameters for the assessment of LVDD.

Methods and results We prospectively included 50 patients and classified them into three groups: with DD (DD+, *n* = 15), without (DD−, *n* = 26), and uncertain (DD±, *n* = 9). Diagnosis of DD was based on echocardiographic E/E′, invasive LV end-diastolic pressure, and N-terminal pro-brain natriuretic peptide. CMR was performed at 1.5 T to assess LV and left atrial (LA) morphology, LV diastolic strain rate (SR) by tissue tracking and tagging, myocardial peak velocities by tissue phase mapping, and transmitral inflow profile using phase contrast techniques. Statistics were performed only on definitive DD+ and DD− (total number 41). DD+ showed enlarged LA with LA end-diastolic volume/height performing best to identify DD+ with a cut-off value of ≥0.52 mL/cm (sensitivity = 0.71, specificity = 0.84, and area under the receiver operating characteristic curve = 0.75). DD+ showed significantly reduced radial (inferolateral E peak: DD−: −14.5 ± 6.5%/s vs. DD+: −10.9 ± 5.9%/s, *P* = 0.04; anterolateral A peak: DD−: −4.2 ± 1.6%/s vs. DD+: −3.1 ± 1.4%/s, *P* = 0.04) and circumferential (inferolateral A peak: DD−: 3.8 ± 1.2%/s vs. DD+: 2.8 ± 0.8%/s, *P* = 0.007; anterolateral A peak: DD−: 3.5 ± 1.2%/s vs. DD+: 2.5 ± 0.8%/s, *P* = 0.048) SR in the basal lateral wall assessed by tissue tracking. In the same segments, DD+ showed lower peak myocardial velocity by tissue phase mapping (inferolateral radial peak: DD−: −3.6 ± 0.7 ms vs. DD+: −2.8 ± 1.0 ms, *P* = 0.017; anterolateral longitudinal peak: DD−: −5.0 ± 1.8 ms vs. DD+: −3.4 ± 1.4 ms, *P* = 0.006). Tagging revealed reduced global longitudinal SR in DD+ (DD−: 45.8 ± 12.0%/s vs. DD+: 34.8 ± 9.2%/s, *P* = 0.022). Global circumferential and radial SR by tissue tracking and tagging, LV morphology, and transmitral flow did not differ between DD+ and DD−.

Conclusions Left atrial size and regional quantitative myocardial deformation applying CMR identified best patients with DD.

Keywords Diastolic dysfunction; Cardiovascular magnetic resonance; Tissue tracking; Left atrium; Myocardial deformation; Heart failure with preserved ejection fraction

Received: 29 December 2019; Revised: 9 May 2020; Accepted: 1 June 2020

**Correspondence to: Jeanette Schulz-Menger, Charité—Universitätsmedizin Berlin, corporate member of Freie Universität Berlin, Humboldt-Universität zu Berlin, and Berlin Institute of Health, Working Group on Cardiovascular Magnetic Resonance, Experimental and Clinical Research Center, a joint cooperation between the Charité Medical Faculty and the Max Delbrueck Center for Molecular Medicine, Lindenberger Weg 80, 13125 Berlin, Germany. Tel: +49 30 450 553 746; Fax: +49 30 450 553 949.
Email: jeanette.schulz-menger@charite.de*

Introduction

Heart failure (HF) with preserved ejection fraction (HFpEF) is prevalent in up to 50% of HF patients.[1] According to the 2016 European Society of Cardiology guidelines for the diagnosis and treatment of acute and chronic HF, HFpEF is defined as the presence of symptoms or signs of HF combined with left ventricular ejection fraction (LVEF) $\geq$ 50% and evidence of left ventricular (LV) diastolic dysfunction (DD).[2] In contrast to HF with reduced ejection fraction, survival of HFpEF could not be improved in the last decades, although mortality is comparable between both groups.[1] The causes are complex and still subject of active research. In 2007, it was recommended to diagnose DD based on either invasive quantification of LV end-diastolic pressure or echocardiographic evaluation of LV diastolic function using the ratio (E/E') of early transmitral flow velocity (E) assessed by blood flow Doppler to tissue Doppler-derived early diastolic lengthening velocities (E') or by combination of echocardiographic parameters and N-terminal pro-brain natriuretic peptide as HF biomarker.[2] The non-invasive diagnosis remains challenging, even though different innovative parameters were introduced applying echocardiography[3] as well as cardiovascular magnetic resonance (CMR).

CMR has the capability to identify and differentiate myocardial injury already in preserved ejection fraction as reflected in the recent guidelines of chronic HF.[4] It is also known as the gold standard for assessment of LV volume and function and offers various techniques to characterize the myocardium. Assessment of DD applying CMR is not yet a clinical routine. Different approaches were evaluated and mostly compared with echocardiography as the diagnostic standard.[5,6]

Similar to Doppler echocardiography, CMR is able to quantify transmitral flow using phase contrast (PC) imaging techniques. Early and late diastolic flow velocity peaks can be quantified and used for evaluation of LV diastolic function.[7] CMR tissue phase mapping (TPM) offers the possibility to assess velocities of myocardial deformation.[8] CMR tagging allows the quantification of myocardial strain based on an intrinsic tissue grid generated by magnetization saturation of specific myocardial localizations.[9] Tissue tracking is a recently introduced post-processing method to quantify myocardial strain. It is based on voxel-related quantification of myocardial deformation using standard cine CMR images.[10]

Several studies have demonstrated the applicability of these techniques to evaluate diastolic LV function in both healthy[8,11] and diseased patients,[12–18] using different comparators.

The aim of our study was to evaluate the capability of different CMR parameters and techniques to detect DD.

Methods

Study population

Patients aged between 18 and 85 years with indication for elective left heart catheterization including coronary angiography were screened and prospectively enrolled into the study. Inclusion criterion was a preserved LVEF $\geq$ 50%. Exclusion criteria included common contraindications for CMR, pregnancy, cardiac arrhythmia, left bundle branch block, previously known infarction scars located at the lateral or septal LV wall, pericardial disease, moderate to severe valvular heart disease, history of valvular or bypass surgery, severe liver disease, impaired renal function (estimated glomerular filtration rate <60 mL/min/m^2), severe pulmonary disease ($\geq$COPD GOLD II), pulmonary arterial hypertension, active cancer, or severe infections.

We identified patients with (DD+), without (DD−), or uncertain (DD±) DD according to Paulus *et al.*[2] by quantification of echocardiographic E/E', invasive LV end-diastolic pressure, and N-terminal pro-brain natriuretic peptide (*Figure 1A*). A 6 min walk test was performed to objectify functional exercise capacity according to the guidelines of the American Thoracic Society. We aimed at completing the whole study protocol within 24 h (*Figure 1B*).

Written informed consent was obtained from all patients. The study was approved by the institutional ethical board and complies with the Declaration of Helsinki.

Cardiovascular magnetic resonance

CMR was performed on a clinical 1.5 T MR scanner (Avanto, Siemens Healthineers, Erlangen, Germany) using a 12-channel phased-array coil. Image data were acquired electrocardiogram-gated and in end-expiratory breath-hold.

Assessment of the left ventricle and the left atrium

To assess LV and left atrial (LA) morphology and function, we acquired three long-axis (LAX) planes in two-chamber, three-chamber, and four-chamber views of the LV as well as two stacks of short-axis (SAX) views covering the entire LV or LA, respectively, using standard cine steady-state free precession (SSFP) sequences [temporal resolution 34.7 ms; echo time (TE) 1.2 ms; field of view (FOV) 292 × 360 mm^2; LAX: slice thickness 6 mm and matrix 156 × 192//LV SAX: slice thickness 7 mm, spacing 3 mm, and matrix 208 × 256; and LA SAX: slice thickness 5 mm, no gap[19]].

Left ventricular cine images for tissue tracking

Cine SSFP images in LAX four-chamber views and three SAX slices (basal, midventricular, and apical) were acquired with a high temporal resolution of 13.8 ms (TE 1.2 ms, 64 phases,

Figure 1 (A) Study group definition and number of patients. (B) Study protocol. LVEDP, left ventricular end-diastolic pressure; NT-proBNP, N-terminal pro-brain natriuretic peptide.

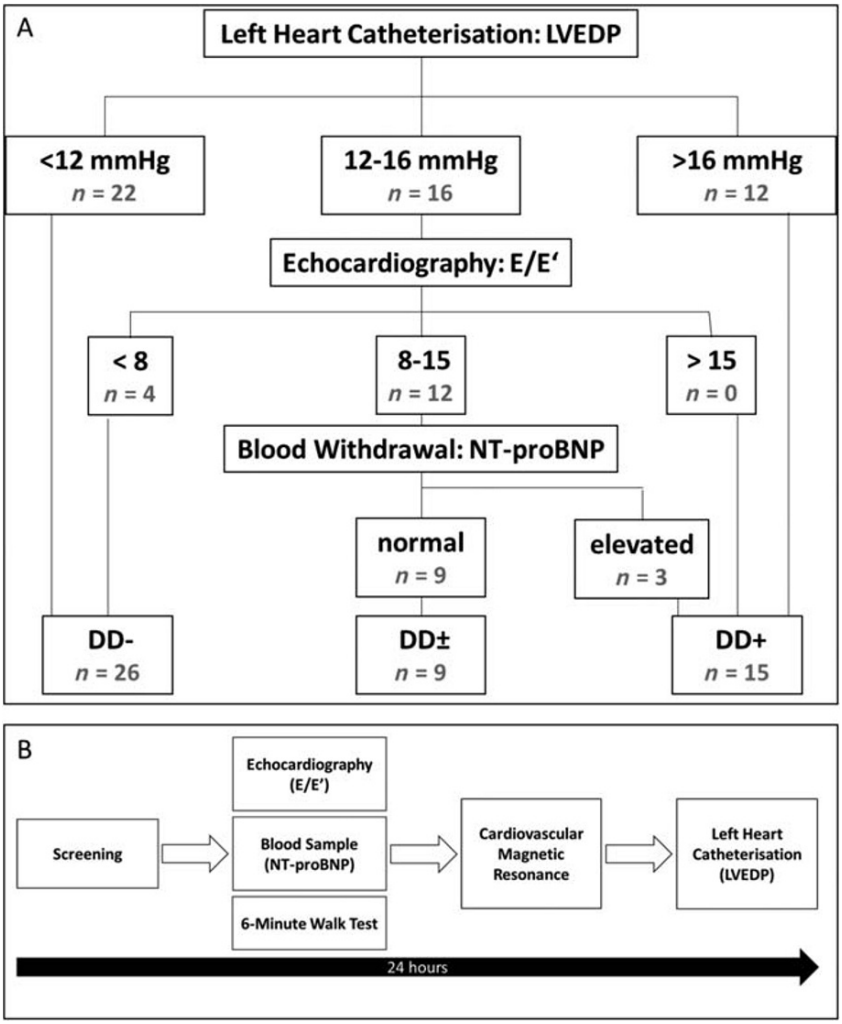

matrix 208 × 256, FOV 325 × 400 mm^2, slice thickness 8 mm, and in-plane resolution 1.6 × 1.6 mm^2) to evaluate diastolic strain rate (SR) by tissue tracking.

Tagging

LAX four-chamber views and three SAX slices (basal, midventricular, and apical) were used to perform SSFP spatial modulation of magnetization (SPAMM) tagging and complementary SPAMM (CSPAMM) tagging for evaluation of diastolic SR (temporal resolution SPAMM/CSPAMM 21.1 ms/42.3 ms, TE 1.3 ms, matrix 256 × 256, FOV 300 × 300 mm^2, slice thickness 6 mm, flip angle 20°, tag spacing 7 mm, and one slice per breath-hold).[20]

Tissue phase mapping

TPM imaging of three SAX slices (basal, midventricular, and apical) was acquired to assess myocardial peak velocities using a black blood prepared gradient echo TPM sequence [temporal resolution of 17.1 ms, TE 3.9 ms, matrix 120 × 160, FOV 255 × 340 mm^2, slice thickness 8 mm, velocity encoding (VENC) in-plane 15 cm/s, VENC through plane 25 cm/s, and one slice per breath-hold].[15]

Phase contrast—transmitral flow

We performed PC imaging in basal SAX positioned at the level of the mitral valve tips during end-diastole and perpendicular to the transmitral inflow to analyse transmitral flow velocities (temporal resolution of 17.4 ms, TE 2.4 ms, 64 phases, matrix 176 × 256, FOV 220 × 320 mm^2, slice thickness 5.5 mm, in-plane resolution 1.3 × 1.3 mm^2, and VENC 120 cm/s). Two more SAX slices were acquired above and below this slice without gap. Each acquisition was repeated a second time.

Post-processing analysis

Assessment of the left ventricle and the left atrium

Analysis of LV and LA morphology was performed with commercially available software (cvi42 Version 4.1.3, Circle Cardiovascular Imaging Inc., Calgary, Canada). LV epicardial and endocardial contours were traced manually in end-systole and end-diastole to assess LV mass (LVM), LV end-diastolic volume (LVEDV) and LV end-systolic volume, LV stroke volume, LVEF, and LV remodelling index as the ratio of LVEDV and LVM.[21,22] Papillary muscles were traced separately.

The stack of LA SAX was analysed similarly. LA systole and LA diastole were defined as phases of minimal or maximal LA dimensions. Pulmonary veins and atrial appendage were excluded.[23] LA minimal and maximum volumes (LA-EDV), LA stroke volume, and LA ejection fraction were assessed. Normalization to body surface area (BSA) and body height (H) was performed for LVM, LVEDV, LV end-systolic volume, and the volumetric LA parameters.

LA area was measured in the LAX cine SSFP images in the two-chamber, three-chamber, and four-chamber views. Pulmonary veins were excluded, and LA appendage was included.[19] Longitudinal and transversal diameters were defined in two-chamber and four-chamber views as well.[19]

Tissue tracking

Two-dimensional tissue tracking was performed using cvi42 prototype 5.3.0 (Circle Cardiovascular Imaging Inc.). End-diastolic contours of LV endocardium and epicardium were defined in all slices excluding papillary muscles. For regional analysis, a basal SAX reference point was set at the anterior insertion of the right ventricle. The deformation analysis was performed automatically. Radial (Err) and circumferential (Ecc) myocardial deformation were evaluated based on SAX analysis, LAX four-chamber view was used to assess longitudinal (Ell) strain parameters. Global preE, E, and A peaks of diastolic SR were defined as shown in *Figure 2C*. SR peaks were determined manually for each slice and each direction of movement.

The analysis was performed both per slice and per segment to identify regional differences. The segmentation was based on the 16-segment model according to the American Heart Association.[24] We excluded the assessment of preE in the regional evaluation but determined the maximum peak (Ecc max and Err max) during the whole diastolic phase (time between aortic valve closure and mitral valve closure). In case of undefinable E and A, only maximum peaks during the whole diastole were assessed.

Tagging

Tagging images were analysed using CIM Tag2D Heart Deformation WIP20 (Heart Deformation post-processing prototype 2.0, Auckland MRI Research Group, University of Auckland, Auckland, New Zealand). LV endocardium and epicardium as well as insertions of the right ventricle were defined in end-diastole. Myocardial tags were contoured semi-automatically in all phases of each slice. To achieve a maximum accordance of image tag lines and overlaid analysing grid, the model stripes were adapted every second (CSPAMM) to fourth (SPAMM) frame using additional guide points.[18] We generated Ecc SR from SAX and Ell SR out of LAX four-chamber view images. Peak diastolic SR was defined as first peak after end-systole. Global and segmental (six segments per slice) analyses were performed.

Tissue phase mapping

Post-processing analysis was performed using MATLAB (The MathWorks, Inc., Natick, MA, USA). Epicardial and endocardial contours were defined semi-automatically for each phase of each slice before starting myocardial velocity measurements as described recently.[15] Peak diastolic radial (Vr) and longitudinal (Vz) velocities were assessed for global and segmental analysis. Regional analysis was based on the 16-segment model according to the American Heart Association.[24]

Phase contrast—transmitral flow

cvi42 (Version 4.1.3, Circle Cardiovascular Imaging Inc.) was used to perform post-processing analysis of PC velocity measurements. The slice showing best the mitral valve tip separation was chosen. Regions of interest were set semi-automatically based on colour-coded display of transmitral blood flow. Early (E) and late (A) diastolic peak velocities were derived from transmitral flow velocity curves. For statistical analysis, we used mean values of repeated measurements of E, A, and the ratio E/A.

Non-diagnostic images due to breath-hold artefacts or malpositioning were excluded.

Statistical analysis

Statistical analyses were performed by relying only on DD+ (n = 15) and DD− (n = 26, i.e. in total 41 patients) groups as our aim was to identify a CMR parameter, which would best meet the published criteria to identify definite DD. Data are shown as mean ± standard deviation. Statistical tests were performed using IBM SPSS Statistics 25 (IBM Corp., Armonk, NY, USA). Mann–Whitney U test was used for analysis of group differences, whereas significance was stated at $P < 0.05$. Correlation analysis was performed using the Spearman correlation coefficient. Receiver operating characteristic (ROC) curve analyses were established to define cut-off values. As the aim of this study was the identification of parameters with discriminatory power, no formal sample size calculation was performed.

Figure 2 Overview cardiovascular magnetic resonance techniques. Left ventricular–midventricular short-axis view of myocardial deformation via tagging in (A1) end-diastole and (A2) end-systole. Left ventricular–midventricular short-axis view of colour-encoded myocardial velocity tissue phase mapping in (B1) end-diastole and (B2) end-systole. Assessment of cardiovascular magnetic resonance tissue tracking: (C1) end-diastolic contouring and tissue tracking and (C2) end-systolic myocardial deformation. (C3) Radial strain and (C4) strain rate: the graphs show phases of one cardiac cycle. The definitions were as follows: end-systole = phase of aortic valve closure; isovolumetric relaxation time (IVRT) = time between end-systole and mitral valve opening; and end-diastole = phase of mitral valve closure. Peaks of myocardial strain rate were defined as follows: (i) preE = peak within IVRT; (ii) E = peak between mitral valve opening and start of diastolic plateau phase; and (iii) A = peak between end of diastolic plateau phase and end-diastole. (D) Stack of short-axis views of left atrial (LA) and contouring in LA diastolic phase. (E) Measurement of LA plane and diameters in long-axis two-chamber, three-chamber, and four-chamber views. (F) Assessment of phase contract transmitral flow velocities: basal short-axis views with and without colour-encoded visualization and contouring of the mitral annulus; transmitral flow velocity curve with early (E) and late (A) diastolic peak velocities.

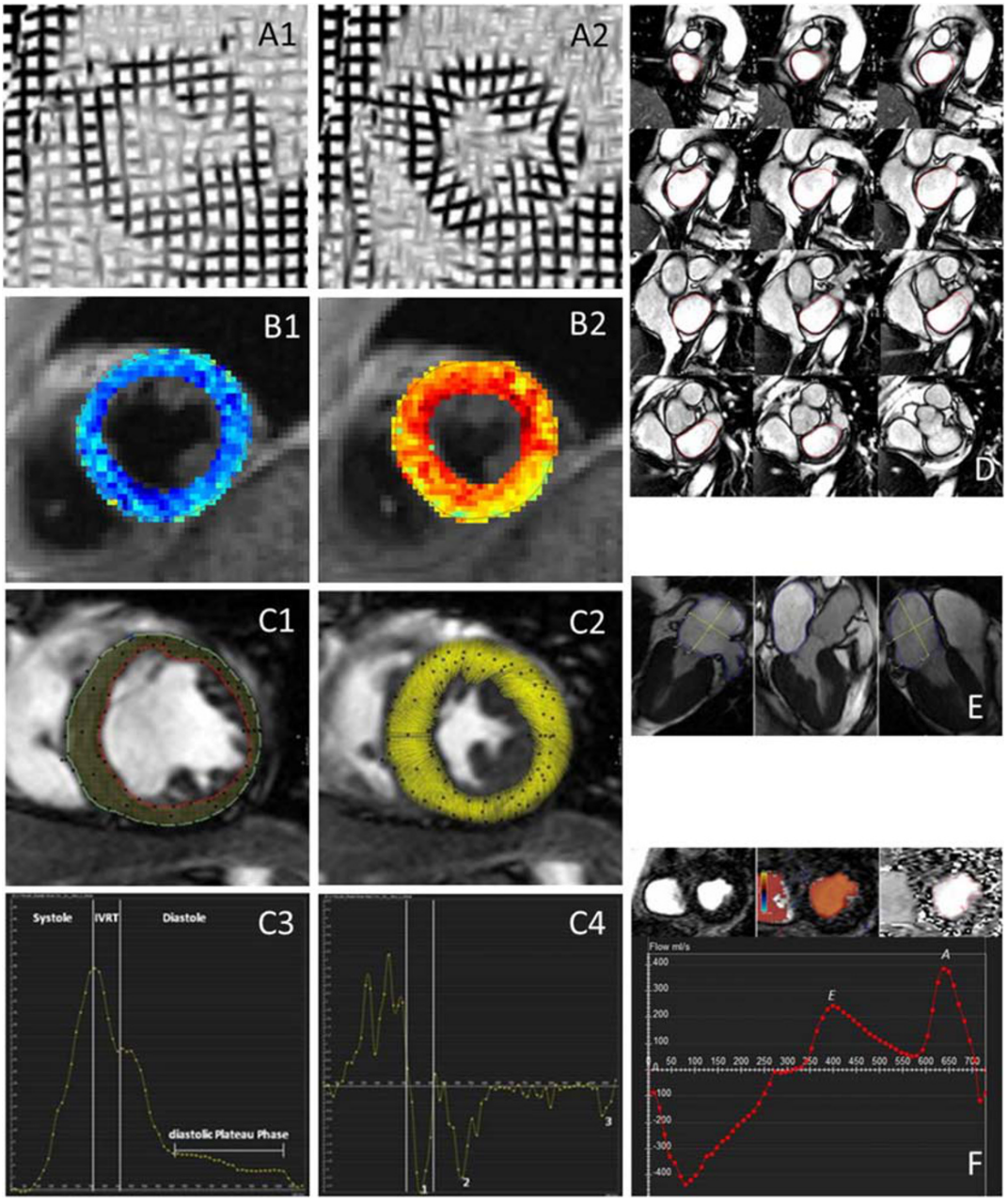

DOI: 10.1002/ehf2.12846

Results

Study population

We screened 741 patients with an indication for LV catheterization between May 2013 and June 2014. Fifty-nine met our criteria and were included, with 39% having their first invasive procedure due to suspected coronary artery disease and 61% having suspicion of progression of their known coronary artery disease. Nine out of these 59 patients dropped out because of arrhythmia, EF < 50% as defined by CMR, claustrophobia, aortic stenosis, or increased LVEDV index, resulting in n = 50 as the final sample. We finally identified 26 DD−, 15 DD+, and 9 DD±. DD+ showed significant higher body mass index compared with DD−. For detailed demographics, see *Table 1*. In 40 out of 50 cases, examinations could be performed within 24 h (mean 25.4 h; range 16.3–91.1 h). Walking distance did not differ significantly between DD+ and DD− (P = 0.129). ROC curve analyses showed an area under the ROC curve (AUC) of 0.663 (*Figure 3*).

Cardiovascular magnetic resonance analysis

Data analysis was performed in all patients. Detailed data are given in Supporting Information, *Tables S1* and *S2*.

Assessment of the left ventricle and the left atrium

Two cases had to be excluded. Results are given in *Table 2*. LV volumes and LVM did not show significant differences between DD+ and DD−.

Left atrial size was larger in DD+ with significantly higher LA-EDV and LA area. The difference remained significant when normalizing to body height. ROC curve analysis (*Figure 3*) showed best results for LA-EDV/H with a cut-off value of ≥0.52 mL/cm (sensitivity = 0.71, specificity = 0.84, AUC = 0.75, and accuracy = 0.75) to differentiate between DD+ and DD−.

Tissue tracking

Five cases had to be excluded. Global analysis did not show significant differences. Results of regional analysis are shown in *Figure 4A*. In 53 out of 992 segments, only maximum peaks during the whole diastole were assessed. DD+ presented impaired E and A with significant reductions in basal inferolateral, anterolateral, and apical anterior segments. Furthermore, Err max of DD+ was significantly lower in the basal anterolateral segment (DD−: −16.5 ± 7.94%/s vs. DD+: −9.8 ± 3.85%/s, P = 0.011).

Tagging

We had to exclude 18 out of 666 segments in SPAMM data and 24 out of 630 segments in CSPAMM data. SPAMM showed reduced global Ell SR in DD+ (DD−: 45.8 ± 12.0%/s vs. DD+: 34.8 ± 9.2%/s, P = 0.022). Further global and segmental amplitude of Ecc and Ell diastolic SR did not differ significantly between DD+ and DD− (*Figure 4C*).

Tissue phase mapping

Forty-four out of 560 mostly apical located segments had to be excluded. The amount of global diastolic peak velocities reached statistical significance in apical Vz (DD−: −2.7 ± 0.6 cm/s vs. DD+: −2.2 ± 1.0 cm/s, P = 0.029). Results of segmental evaluation are visualized in *Figure 4B*. Vz and Vr differ significantly in the basolateral segments.

Table 1 Characteristics of the study population

	Study groups		
	Without diastolic dysfunction (DD−)	Uncertain diastolic function (DD±)	With diastolic dysfunction (DD+)
Sample size (n)	26	9	15
Sex (male|female)	16|10	9|0	9|6
Age (years)	66.6 ± 8.9	68.0 ± 7.3	70.5 ± 7.4
BMI (kg/m^2)	26.7 ± 3.0	28.6 ± 4.7	29.7 ± 3.2*
6MWD (m)	509 ± 76	487 ± 114	446 ± 122
LVEDP (mmHg)	8 ± 3	14 ± 1*	20 ± 5*†
E/E′	8.5 ± 2.0	10.8 ± 1.4*	10.1 ± 2.0*
NT-proBNP (ng/mL)	184 ± 151	157 ± 107*	447 ± 422*
Heart rate (b.p.m.)	68 ± 11	70 ± 11	64 ± 8
Arterial hypertension (%)	84.6	100.0	93.3
Coronary artery disease (%)	88.5	100.0	80.0
One-vessel disease (%)	23.1	33.3	26.7
Two-vessel disease (%)	34.6	55.6	20.0
Three-vessel disease (%)	30.8	11.1	33.3
Diabetes mellitus (%)	34.6	11.1	33.3
Hyperlipoproteinaemia (%)	38.5	66.7	60.0

6MWD, 6 min walking distance; BMI, body mass index; E/E′, ratio of early transmitral flow velocity (E) and early diastolic lengthening velocity (E′); LVEDP, left ventricular end-diastolic pressure; NT-proBNP, N-terminal pro-brain natriuretic peptide.
Data are shown as mean ± standard deviation.
*For P < 0.05 compared with DD−.
†For P < 0.05 compared with DD±.

Figure 3 Diagnostic performance of measurements of the left atrium and walking distance to identify diastolic dysfunction. (A) Receiver operating characteristic curves of left atrial (LA) end-diastolic volume (EDV), area of three-chamber view, and triplane mean area indexed to height (H). (B) Receiver operating characteristic curve of walking distance assessed by 6 min walk test.

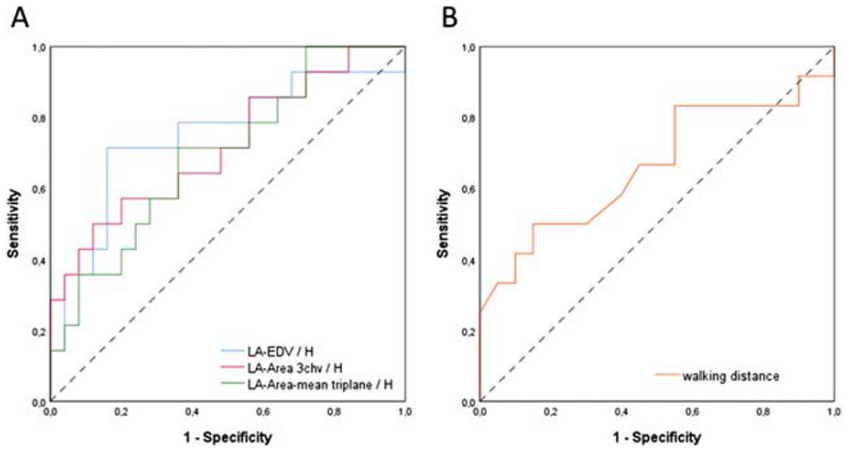

Table 2 Findings of LV and LA analysis of DD− and DD+

	DD−	DD+	*P*-value
Left ventricle			
LVEDV (mL)	122.6 ± 34.3	130.5 ± 32.4	0.429
LVEDV/BSA (mL/m^2)	63.7 ± 14.0	66.3 ± 14.9	0.639
LV-SV (mL)	83.3 ± 21.3	86.0 ± 22.2	0.548
LVEF (%)	69.0 ± 7.6	66.0 ± 7.4	0.334
LVM (g)	96.5 ± 29.9	110.2 ± 30.6	0.092
LVM/H (g/cm)	0.6 ± 0.1	0.7 ± 0.2	0.050
LVM/BSA (g/m^2)	49.9 ± 11.3	55.6 ± 12.3	0.079
LVRI (g/mL)	0.8 ± 0.1	0.9 ± 0.2	0.412
Left atrium—quantification based on full coverage (volume)			
LA-EDV (mL)	74.4 ± 17.2	93.3 ± 26.2	0.014*
LA-EDV/H (mL/cm)	0.4 ± 0.1	0.6 ± 0.1	0.010*
LA-EDV/BSA (mL/m^2)	39.2 ± 8.9	46.6 ± 12.0	0.069
LA-SV (mL)	38.7 ± 8.4	41.2 ± 13.0	0.578
LAEF (%)	52.7 ± 7.4	45.7 ± 13.1	0.151
Left atrium—quantification based on area			
LA area 4CV (mm^2)	20.1 ± 6.2	22.1 ± 5.4	0.169
LA area 4CV/H (mm^2/cm)	0.12 ± 0.03	0.13 ± 0.03	0.188
LA area 3CV (mm^2)	18.6 ± 3.8	22.3 ± 5.9	0.033*
LA area 3CV/H (mm^2/cm)	0.11 ± 0.02	0.13 ± 0.03	0.026*
LA area 2CV (mm^2)	20.4 ± 5.5	24.8 ± 5.6	0.035*
LA area 2CV/H (mm^2/cm)	0.12 ± 0.03	0.15 ± 0.03	0.061
LA area mean biplane (mm^2)	20.2 ± 5.5	23.5 ± 4,8	0.084
LA area mean biplane/H (m^2/cm)	0.12 ± 0.03	0.14 ± 0.03	0.079
LA area mean triplane (mm^2)	19.7 ± 4.6	23.1 ± 5.1	0.084
LA area mean triplane/H (m^2/cm)	0.12 ± 0.03	0.13 ± 0.03	0.046*

2/3/4CV, two-chamber/three-chamber/four-chamber view; BSA, body surface area; DD−, patients without diastolic dysfunction; DD+, patients with diastolic dysfunction; EDV, end-diastolic volume; H, body height; LA, left atrial; LAEF, left atrial ejection fraction; LV, left ventricular; LVEF, left ventricular ejection fraction; LVM, left ventricular mass; LVRI, left ventricular remodelling index; SV, stroke volume.
Data are shown as mean ± standard deviation.
*For $P < 0.05$.

Phase contrast—transmitral flow

For assessment of transmitral flow, two cases had to be excluded. Neither E (DD−: 0.5 ± 0.1 cm/s vs. DD+: 0.5 ± 0.1 cm/s, $P = 0.689$) nor A (DD−: 0.6 ± 0.2 cm/s vs. DD+: 0.6 ± 0.2 cm/s, $P = 0.753$) or E/A (DD−: 0.8 ± 0.3 vs. DD+: 1.1 ± 0.9, $P = 0.441$) differed significantly between DD− and DD+.

Discussion

CMR provides various techniques to assess cardiac structure and function.[25] In this study, we are providing for the first time a comparison of CMR parameters of diastolic function with a published gold standard including invasive measurements. Based on the quantification of LA size, a cut-off can be derived to identify

Figure 4 Regional myocardial differences between patients with and without diastolic dysfunction. Significant differences are highlighted in red. (A) Tissue tracking: early (E) and atrial (A) diastolic peaks of circumferential and radial strain rate ± standard deviation. *P*-values of segments showing significant differences are Ecc A peak: basal inferolateral ($P = 0.007$) and apical anterior ($P = 0.014$); Err E peak: basal inferolateral ($P = 0.030$); and Err A peak: basal inferolateral ($P = 0.033$) and apical anterior ($P = 0.019$). (B) Tissue phase mapping (TPM) radial and longitudinal peak diastolic velocities ± standard deviation. *P*-values of segments showing significant differences are Vr basal inferolateral ($P = 0.018$), Vz basal anterolateral ($P = 0.007$), and Vz medial anterior ($P = 0.044$). (C) Tagging [spatial modulation of magnetization (SPAMM) and complementary spatial modulation of magnetization (CSPAMM)]: diastolic peak of circumferential strain rate ± standard deviation.

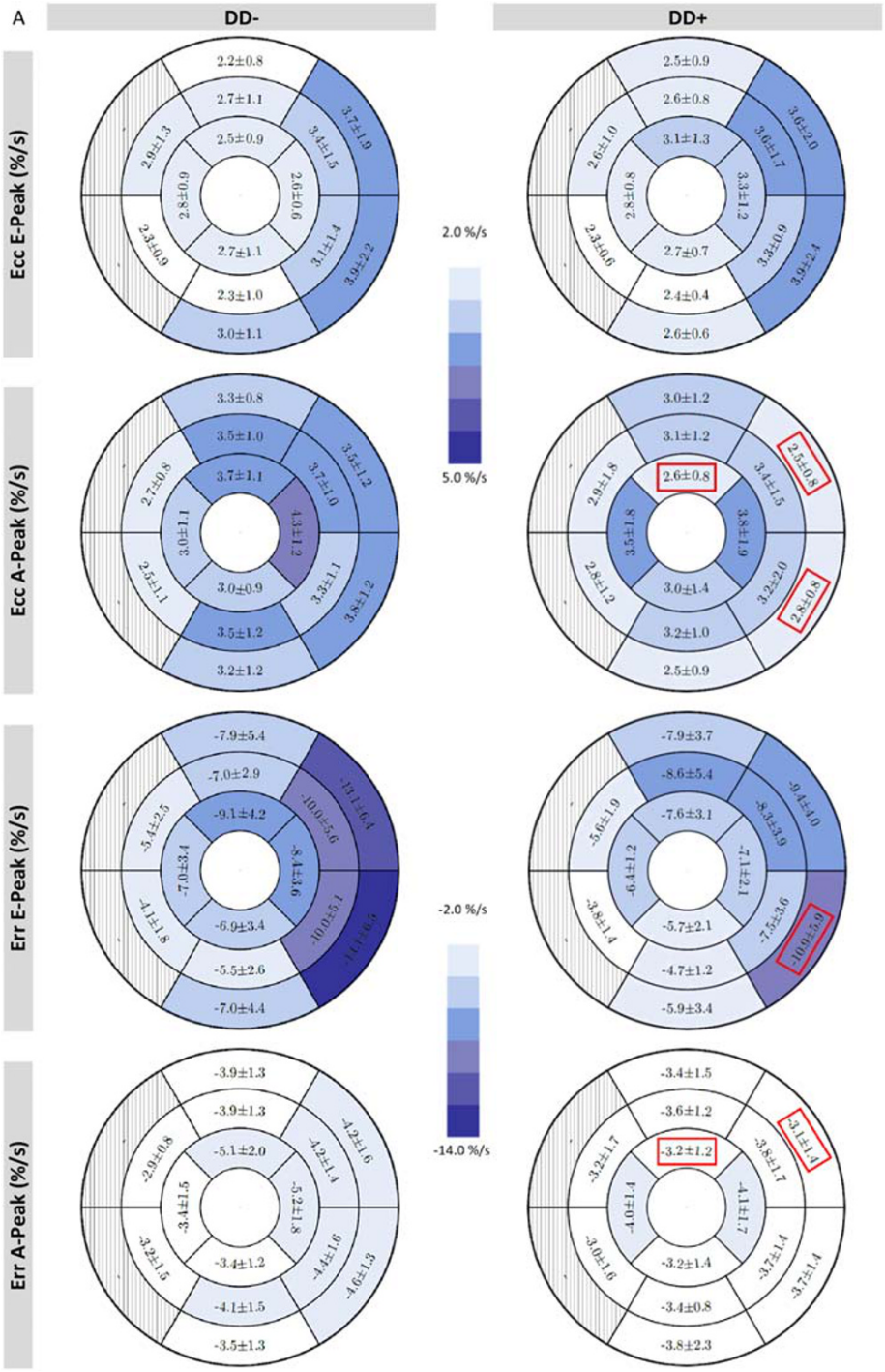

Figure 4 Continued

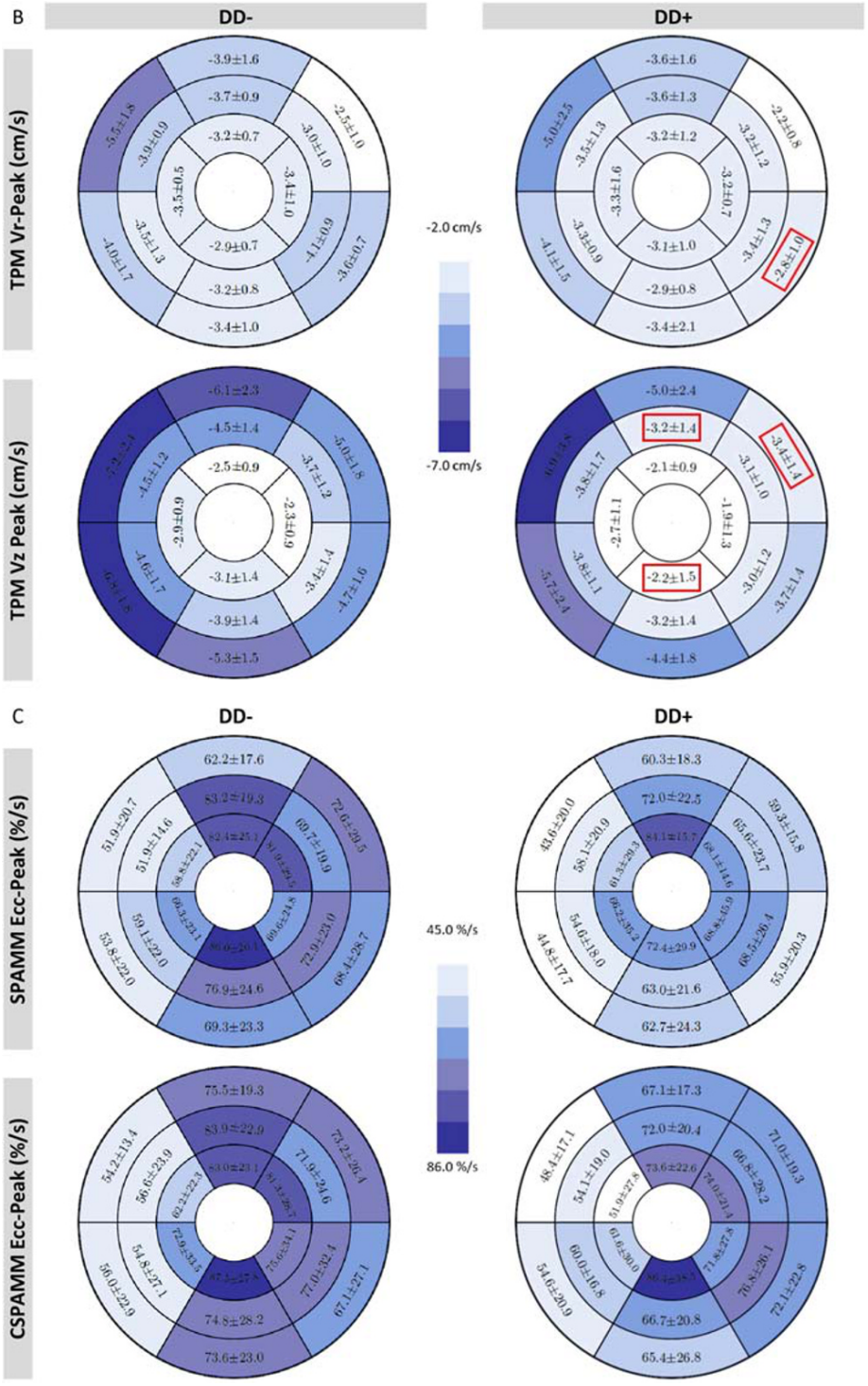

DD. Furthermore, quantification of diastolic LV deformation has been found to be predictive to identify patients with DD.

Specifically, our main findings are as follows:

i Enlarged LA dimensions of LA-EDV/H $\geq$ 0.52 mL/cm have a diagnostic accuracy of 0.75 (AUC = 0.75) on our data to identify DD.
ii Tissue tracking and TPM reveal impaired diastolic deformation of the basal lateral wall in DD+ as a direct sign of DD.

LA enlargement is well known in LVDD, caused by a chronic increase of LV filling pressure due to impaired relaxation and reduced compliance.[26] LA dilatation already is part of the diagnostic algorithm of DD in both the consensus statement of the Heart Failure and Echocardiography Association of the European Society of Cardiology published in 2007[2] and the current recommendations of the American Society of Echocardiography and the European Association of Cardiovascular Imaging published in 2016.[3] They recommended cut-off values of 40 and 34 mL/m^2, respectively, for echocardiographic LA maximal volume indexed to BSA. LA-EDV/BSA did not show significant differences between DD+ and DD− in our study. Compared with the echocardiographic cut-offs, both groups reached borderline or higher mean values (DD−: 39.2 ± 8.9 mL/m^2 vs. DD+: 46.6 ± 12.0 mL/m^2), but echocardiography is known to show systematically smaller LA volumes as compared with CMR.[27] Furthermore, our DD+ group had a significantly higher body mass index than DD−. Patel *et al*.[28] showed that LA-EDV/BSA underestimates the prevalence of LA enlargement in obese populations, whereas the level of obesity did not affect indices to height. As increased LA volume is associated with prognosis and cardiovascular events,[26] investigation of LA size is of general importance. But enlarged LA size is correlated with both HFpEF and HF with reduced EF.[29]

In our study, LA volume quantification was based on the evaluation of a stack of SAX as reported by Maceira *et al*.[19] In principle, it could also be assessed by reliance on transverse slices, which is mainly used in congenital heart disease and has also recently been applied in the detection of subclinical atrial fibrillation.[30,31] As a consequence, more subtle differences that might be captured by transverse slices may have been missed. Currently, there are no head-to-head comparisons published regarding superiority, for example, to predict outcome. Unfortunately, constraints in scan time did not allow to collect scans in the transverse orientation. If scan time is limited, it is also acceptable to assess LA volume by two-dimensional area-length method.[23]

A 6 min walk test is one of the most popular clinical exercise tests.[32] It is often used to objectify and compare functional exercise capacity between different groups or before and after medical interventions. In our study, walking distance did not differ significantly between DD+ and DD−. Furthermore, ROC curve analyses showed numerically better diagnostic ability for LA-EDV/H than walking distance without reaching statistical significance.

Echocardiographic E and A peaks of transmitral flow are part of the clinical standard for estimating LV filling pressure and grading DD.[3] PC imaging is able to assess blood flow velocities.[7] Our study was not designed to compare equivalent echocardiographic and CMR parameters. But previous studies showed good correlation between echocardiographic and CMR-derived parameters and a general underestimation of transmitral flow parameters by CMR.[33–35] In our study, E and A peaks as well as E/A ratio did not differ significantly between DD+ and DD−. Graca *et al*. studied 48 healthy volunteers using CMR and detected a higher prevalence of DD in men than in women. They defined and graded DD by PC CMR-derived transmitral E/A ratio, mitral deceleration time, and LA size.[36]

Changes in LA morphology and transmitral flow patterns merely represent a consequence of DD. One would expect that the evaluation of intrinsic myocardial characteristics offers new insights into DD. In echocardiography, global longitudinal SR is a frequently applied parameter to evaluate diastolic function and also known for the assessment of systolic function. It is known to have a significant association with the time constant of LV relaxation and has been used to predict outcomes in several disease stages.[3] In our study, we found significantly reduced Ell SR assessed by tagging SPAMM in DD+. Because of technical limitations, tissue tracking-derived Ell SR was not reliable in our setting. Future technical improvements may overcome these limitations.

On the other hand, CMR offers a wide spectrum of additional parameters to assess diastolic myocardial deformation applying tagging, tissue tracking, and TPM. Several studies examined applicability of CMR tagging to evaluate diastolic function using different diastolic parameters. We focused on peak early diastolic SR. Diastolic Ecc did not show significant differences between DD+ and DD−. In contrast, both Ennis *et al*.[17] and Edvardsen *et al*.[16] detected significantly decreased early diastolic Ecc SR in patients suffering from familial hypertrophic cardiomyopathy or LV hypertrophy, respectively. Among other reasons, these divergent findings may be due to different study populations, variable degrees of cardiac remodelling, and technical issues including the use of different approaches.

Tissue tracking is a recently introduced post-processing technique to evaluate myocardial strain and SR based on SSFP cine images.[10] Segmental analysis of E and A peak Ecc and Err diastolic SR showed significant reduction in DD+ in the basal lateral wall. Kuetting *et al*.[12] evaluated global midventricular early and peak diastolic Ecc SR in patients with echocardiographically diagnosed DD and controls. Both parameters appeared significantly reduced in patients with DD. We did not find similar differences on the midventricular level of global Ecc. However, healthy controls in the study by Kutting *et al*. were younger and Ecc early diastolic SR has been

shown to decrease with age.[11] For this method, comparison across studies may be misleading as most studies are focusing on systolic strain and SR as well as due to technical reasons and different approaches.[11,12,37] Similar challenges are known from other imaging techniques.[38,39] A comparison with healthy volunteers could help to interpret the published literature, but currently published normal values for segmental diastolic SR analysis based on tissue tracking or tagging are lacking.

The findings in the basal lateral wall using tissue tracking are supported by the TPM results of our study. TPM has been shown to be a reliable technique to evaluate and discriminate myocardial velocities of healthy volunteers and patients.[8] The present study demonstrated impaired Vz in the apical slice. These findings could only partially be reproduced in a segmental analysis. In contrast, we found significantly reduced regional diastolic peak velocities again in the basal lateral wall of DD+. Von Knobelsdorff-Brenkenhoff *et al*.[15] and Foell *et al*.[13] analysed TPM-derived myocardial velocities in healthy volunteers and patients with hypertensive heart disease and preserved EF. Both studies found significantly reduced diastolic Vr and Vz peak velocities in patients. We did not include healthy volunteers, but patients without signs for DD that may explain the differing results. The reduced peak velocities might be caused by the predominant presence of arterial hypertension and higher age. Diastolic Vz and Vr are known to decrease in the elderly.[8] However, the differentiation of age-dependent reduced relaxation and pathological DD is essential and needs further attention in an ageing society. Potentially, reduced diastolic peak velocities in the basal lateral wall play a particular role in this differentiation.

In our cohort, reduced myocardial deformation was mainly detected in the basal lateral segments. Several types of cardiomyopathy like viral myocarditis[40,41] and myocardial dystrophies such as myotonic dystrophy type 2,[42] facioscapulohumeral muscular dystrophy 1,[43] and Becker muscular dystrophy[44,45] show focal and subclinical diffuse fibrosis predominantly in the inferolateral wall. Both focal and diffuse fibrosis have also been seen in HF with preserved ejection fraction or hypertensive heart disease.[21,46] Furthermore, the myocardial deformation response to isometric exercise in subjects with hypertensive heart disease was predominantly abnormal in the lateral segments.[15] Taken together, there is evidence that the inferolateral wall may be a region of early or increased vulnerability for pathological structural and functional changes even though up to now a mechanistic explanation for this observation is lacking.

To underpin our findings of LA enlargement and impairment of diastolic function in the basal lateral wall, a reclassification would have been desirable. But DD± was limited by a small sample size due to missing data regarding group defining measurements (n = 4) and exclusions due to technical reasons (see Supporting Information, *Table S3*). Therefore, the group of DD± would not have been sufficient to perform a reclassification.

Beyond the detection of DD itself, graduation of DD could offer more insights in disease staging and pathophysiology. Our approach did not focus on grading DD and therefore patients with Grade I DD were probably missed or went undetected. The identification of borderline cases and parameters for reclassification should be addressed in future studies.

Irrespective of a potential future implementation of our parameters to clinical practice, transthoracic echocardiography will remain the first-line method to evaluate diastolic function. But in cases of primarily performed CMR, for example, in patients with suspected cardiomyopathy, it may be useful to being able to reliably assess diastolic function as an additional parameter. CMR scans have to be time efficient in clinical routine, which enhances the potential role of a fast biplane LA-EDV/H assessment and tissue tracking analyses with no need for additional image acquisitions.

The present study shows some limitations. First, study results are based on a small sample size even though demographic confounders could be excluded. Second, the definition of study groups was based on the consensus statement by Paulus *et al*.,[2] which shows some minor deviation to the updated recommendations for evaluation of LV diastolic function by echocardiography,[3] which were published after realization of the study. Third, we had not the possibility to run invasive measurements in healthy volunteers; only patients with clinical indication for left heart catheterization were screened. As a consequence, by study design, a group of healthy volunteers with definitive normal diastolic function is lacking in the current study.

In conclusion, CMR is able to identify patients with DD. Enlarged LA is most predictive for DD among evaluated comprehensive CMR parameters. TPM and tissue tracking reflect intrinsic aberration by revealing impaired deformation patterns in the basal lateral segments in comparison with patients with normal diastolic function.

Acknowledgements

We sincerely thank Joost P. A. Kuijer for providing his CMR tagging sequences, Carsten Schwenke for supporting in the statistical analysis, Thomas Grandy for his helpful comments and careful reading, the technicians Kerstin Kretschel, Evelyn Polzin, and Denise Kleindienst for acquiring the CMR data, and the study nurse Annette Köhler-Rhode for assisting in the organization of the CMR scans.

Conflict of interest

A.G. reports personal fees from Siemens Healthcare GmbH, outside the submitted work. P.B. is an employee of Circle

Cardiovascular Imaging Inc. The other authors declare no conflicts of interest.

Funding

J.S.-M. is holding institutional grants of the Charité—Universitätsmedizin Berlin.

Supporting information

Additional supporting information may be found online in the Supporting Information section at the end of the article.

Table S1. Strain rate, myocardial velocity, LV-, LA- and transmitral flow- analysis per slice
Table S2. Findings of regional strain rate and myocardial velocity analysis of DD+ and DD-.
Table S3. Causes for exclusion of cases.

References

1. Owan TE, Hodge DO, Herges RM, Jacobsen SJ, Roger VL, Redfield MM. Trends in prevalence and outcome of heart failure with preserved ejection fraction. *N Engl J Med* 2006; **355**: 251–259.
2. Paulus WJ, Tschöpe C, Sanderson JE, Rusconi C, Flachskampf FA, Rademakers FE, Marino P, Smiseth OA, De Keulenaer G, Leite-Moreira AF, Borbély A. How to diagnose diastolic heart failure: a consensus statement on the diagnosis of heart failure with normal left ventricular ejection fraction by the Heart Failure and Echocardiography Associations of the European Society of Cardiology. *Eur Heart J* 2007; **28**: 2539–2550.
3. Nagueh SF, Smiseth OA, Appleton CP, Byrd BF, Dokainish H, Edvardsen T, Flachskampf FA, Gillebert TC, Klein AL, Lancellotti P, Marino P. Recommendations for the evaluation of left ventricular diastolic function by echocardiography: an update from the American Society of Echocardiography and the European Association of Cardiovascular Imaging. *J Am Soc Echocardiography* 2016; **29**: 277–314.
4. Ponikowski P, Voors AA, Anker SD, Bueno H, Cleland JG, Coats AJ, Falk V, González-Juanatey JR, Harjola VP, Jankowska EA, Jessup M, Linde C, Nihoyannopoulos P, Parissis JT, Pieske B, Riley JP, Rosano GM, Ruilope LM, Ruschitzka F, Rutten FH, van der Meer P. 2016 ESC guidelines for the diagnosis and treatment of acute and chronic heart failure. *Kardiol Pol* 2016; **74**: 1037–1147.
5. Paelinck BP, de Roos A, Bax JJ, Bosmans JM, van Der Geest RJ, Dhondt D, Parizel PM, Vrints CJ, Lamb HJ. Feasibility of tissue magnetic resonance imaging: a pilot study in comparison with tissue Doppler imaging and invasive measurement. *J Am Coll Cardiol* 2005; **45**: 1109–1116.
6. Jung B, Schneider B, Markl M, Saurbier B, Geibel A, Hennig J. Measurement of left ventricular velocities: phase contrast MRI velocity mapping versus tissue-Doppler-ultrasound in healthy volunteers. *J Cardiovasc Magn Reson* 2004; **6**: 777–783.
7. Duarte R, Fernandez G. Assessment of left ventricular diastolic function by MR: why, how and when. *Insights Imaging* 2010; **1**: 183–192.
8. Foll D, Jung B, Schilli E, Staehle F, Geibel A, Hennig J, Bode C, Markl M. Magnetic resonance tissue phase mapping of myocardial motion: new insight in age and gender. *Circ Cardiovasc Imaging* 2010; **3**: 54–64.
9. Ibrahim el SH. Myocardial tagging by cardiovascular magnetic resonance: evolution of techniques—pulse sequences, analysis algorithms, and applications. *J Cardiovasc Magn Reson* 2011; **13**: 36.
10. Ortega M, Triedman JK, Geva T, Harrild DM. Relation of left ventricular dyssynchrony measured by cardiac magnetic resonance tissue tracking in repaired tetralogy of fallot to ventricular tachycardia and death. *Am J Cardiol* 2011; **107**: 1535–1540.
11. Andre F, Steen H, Matheis P, Westkott M, Breuninger K, Sander Y, Kammerer R, Galuschky C, Giannitsis E, Korosoglou G, Katus HA, Buss SJ. Age- and gender-related normal left ventricular deformation assessed by cardiovascular magnetic resonance feature tracking. *J Cardiovasc Magn Reson* 2015; **17**: 25.
12. Kuetting D, Sprinkart AM, Doerner J, Schild H, Thomas D. Comparison of magnetic resonance feature tracking with harmonic phase imaging analysis (CSPAMM) for assessment of global and regional diastolic function. *Eur J Radiol* 2015; **84**: 100–107.
13. Foell D, Jung B, Germann E, Staehle F, Bode C, Markl M. Hypertensive heart disease: MR tissue phase mapping reveals altered left ventricular rotation and regional myocardial long-axis velocities. *Eur Radiol* 2013; **23**: 339–347.
14. Jung B, Foll D, Bottler P, Petersen S, Hennig J, Markl M. Detailed analysis of myocardial motion in volunteers and patients using high-temporal-resolution MR tissue phase mapping. *JMRI* 2006; **24**: 1033–1039.
15. von Knobelsdorff-Brenkenhoff F, Hennig P, Menza M, Dieringer MA, Foell D, Jung B, Schulz-Menger J. *Myocardial dysfunction in patients with aortic stenosis and hypertensive heart disease assessed by MR tissue phase mapping*. JMRI: Journal of magnetic resonance imaging; 2015.
16. Edvardsen T, Rosen BD, Pan L, Jerosch-Herold M, Lai S, Hundley WG, Sinha S, Kronmal RA, Bluemke DA, Lima JAC. Regional diastolic dysfunction in individuals with left ventricular hypertrophy measured by tagged magnetic resonance imaging—the Multi-Ethnic Study of Atherosclerosis (MESA). *Am Heart J* 2006; **151**: 109–114.
17. Ennis DB, Epstein FH, Kellman P, Fananapazir L, McVeigh ER, Arai AE. Assessment of regional systolic and diastolic dysfunction in familial hypertrophic cardiomyopathy using MR tagging. *Magn Reson Med* 2003; **50**: 638–642.
18. Moody WE, Taylor RJ, Edwards NC, Chue CD, Umar F, Taylor TJ, Ferro CJ, Young AA, Townend JN, Leyva F, Steeds RP. Comparison of magnetic resonance feature tracking for systolic and diastolic strain and strain rate calculation with spatial modulation of magnetization imaging analysis. *JMRI* 2015; **41**: 1000–1012.
19. Maceira AM, Cosin-Sales J, Roughton M, Prasad SK, Pennell DJ. Reference left atrial dimensions and volumes by steady state free precession cardiovascular magnetic resonance. *J Cardiovasc Magn Reson* 2010; **12**: 65.
20. Zwanenburg JJ, Kuijer JP, Marcus JT, Heethaar RM. Steady-state free precession with myocardial tagging: CSPAMM in a single breathhold. *Magn Reson Med* 2003; **49**: 722–730.
21. Schulz-Menger J, Abdel-Aty H, Rudolph A, Elgeti T, Messroghli D, Utz W, Boyé P, Bohl S, Busjahn A, Hamm B, Dietz R. Gender-specific differences in left ventricular remodelling and fibrosis in hypertrophic cardiomyopathy: insights

from cardiovascular magnetic resonance. *Eur J Heart Fail* 2008; **10**: 850–854.
22. Schulz-Menger J, Bluemke DA, Bremerich J, Flamm SD, Fogel MA, Friedrich MG, Kim RJ, von Knobelsdorff-Brenkenhoff F, Kramer CM, Pennell DJ, Plein S, Nagel E. Standardized image interpretation and post processing in cardiovascular magnetic resonance: Society for Cardiovascular Magnetic Resonance (SCMR) Board of Trustees Task Force on Standardized Post Processing. *J Cardiovasc Magn Reson* 2013; **15**: 35.
23. Funk S, Kermer J, Doganguezel S, Schwenke C, von Knobelsdorff-Brenkenhoff F, Schulz-Menger J. Quantification of the left atrium applying cardiovascular magnetic resonance in clinical routine. *SCJ* 2018: 1–8.
24. Cerqueira MD, Weissman NJ, Dilsizian V, Jacobs AK, Kaul S, Laskey WK, Pennell DJ, Rumberger JA, Ryan T, Verani MS, Myoca AHAWG. Standardized myocardial segmentation and nomenclature for tomographic imaging of the heart. A statement for healthcare professionals from the Cardiac Imaging Committee of the Council on Clinical Cardiology of the American Heart Association. *Circulation* 2002; **105**: 539–542.
25. Buckberg G, Hoffman JI, Mahajan A, Saleh S, Coghlan C. Cardiac mechanics revisited: the relationship of cardiac architecture to ventricular function. *Circulation* 2008; **118**: 2571–2587.
26. Tsang TS, Barnes ME, Gersh BJ, Bailey KR, Seward JB. Left atrial volume as a morphophysiologic expression of left ventricular diastolic dysfunction and relation to cardiovascular risk burden. *Am J Cardiol* 2002; **90**: 1284–1289.
27. Madueme PC, Mazur W, Hor KN, Germann JT, Jefferies JL, Taylor MD. Comparison of area-length method by echocardiography versus full-volume quantification by cardiac magnetic resonance imaging for the assessment of left atrial volumes in children, adolescents, and young adults. *Pediatr Cardiol* 2014; **35**: 645–651.
28. Patel DA, Lavie CJ, Gilliland Y, Shah S, Ventura H, Milani R. Abstract 712: Left atrial volume and mortality prediction: does the method of indexing matter? *Circulation* 2009; **120**: S382-S.
29. Upadhya B, Taffet GE, Cheng CP, Kitzman DW. Heart failure with preserved ejection fraction in the elderly: scope of the problem. *J Mol Cell Cardiol* 2015; **83**: 73–87.
30. Bertelsen L, Diederichsen SZ, Haugan KJ, Brandes A, Graff C, Krieger D, Kronborg C, Køber L, Højberg S, Vejlstrup N, Svendsen JH. Left atrial volume and function assessed by cardiac magnetic resonance imaging are markers of subclinical atrial fibrillation as detected by continuous monitoring. *Europace* 2020.
31. Wandelt LK, Kowallick JT, Schuster A, Wachter R, Stümpfig T, Unterberg-Buchwald C, Steinmetz M, Ritter CO, Lotz J, Staab W. Quantification of left atrial volume and phasic function using cardiovascular magnetic resonance imaging—comparison of biplane area-length method and Simpson's method. *Int J Cardiovasc Imaging* 2017; **33**: 1761–1769.
32. ATS statement: guidelines for the six-minute walk test. *Am J Respir Crit Care Med* 2002; **166**: 111–117.
33. Rathi VK, Doyle M, Yamrozik J, Williams RB, Caruppannan K, Truman C, Vido D, Biederman RWW. Routine evaluation of left ventricular diastolic function by cardiovascular magnetic resonance: a practical approach. *J Cardiovasc Magn Reson* 2008; **10**: 36.
34. Bollache E, Redheuil A, Clément-Guinaudeau S, Defrance C, Perdrix L, Ladouceur M, Lefort M, de Cesare A, Herment A, Diebold B, Mousseaux E. Automated left ventricular diastolic function evaluation from phase-contrast cardiovascular magnetic resonance and comparison with Doppler echocardiography. *J Cardiovasc Magn Reson* 2010; **12**: 63.
35. Rubinshtein R, Glockner JF, Feng D, Araoz PA, Kirsch J, Syed IS, Oh JK. Comparison of magnetic resonance imaging versus Doppler echocardiography for the evaluation of left ventricular diastolic function in patients with cardiac amyloidosis. *Am J Cardiol* 2009; **103**: 718–723.
36. Graca B, Ferreira MJ, Donato P, Castelo-Branco M, Caseiro-Alves F. Cardiovascular magnetic resonance imaging assessment of diastolic dysfunction in a population without heart disease: a gender-based study. *Eur Radiol* 2014; **24**: 52–59.
37. Taylor RJ, Moody WE, Umar F, Edwards NC, Taylor TJ, Stegemann B, Townend JN, Hor KN, Steeds RP, Mazur W, Leyva F. Myocardial strain measurement with feature-tracking cardiovascular magnetic resonance: normal values. *Eur Heart J Cardiovasc Imaging* 2015; **16**: 871–881.
38. Farsalinos KE, Daraban AM, Unlu S, Thomas JD, Badano LP, Voigt JU. Head-to-head comparison of global longitudinal strain measurements among nine different vendors: the EACVI/ASE Inter-Vendor Comparison Study. *J Am Soc Echocardiogr* 2015; **28**: 1171–1181 e2.
39. Messroghli DR, Moon JC, Ferreira VM, Grosse-Wortmann L, He T, Kellman P, Mascherbauer J, Nezafat R, Salerno M, Schelbert EB, Taylor AJ, Thompson R, Ugander M, van Heeswijk R, Friedrich MG. Clinical recommendations for cardiovascular magnetic resonance mapping of T1, T2, T2* and extracellular volume: a consensus statement by the Society for Cardiovascular Magnetic Resonance (SCMR) endorsed by the European Association for Cardiovascular Imaging (EACVI). *J Cardiovasc Magn Reson* 2017; **19**: 75.
40. Aquaro GD, Perfetti M, Camastra G, Monti L, Dellegrottaglie S, Moro C, Pepe A, Todiere G, Lanzillo C, Scatteia A, di Roma M, Pontone G, Perazzolo Marra M, Barison A, di Bella G, Cardiac Magnetic Resonance Working Group of the Italian Society of Cardiology. Cardiac MR with late gadoslinium enhancement in acute myocarditis with preserved systolic function: ITAMY study. *J Am Coll Cardiol* 2017; **70**: 1977–1987.
41. Mahrholdt H, Wagner A, Deluigi CC, Kispert E, Hager S, Meinhardt G, Vogelsberg H, Fritz P, Dippon J, Bock CT, Klingel K, Kandolf R, Sechtem U. Presentation, patterns of myocardial damage, and clinical course of viral myocarditis. *Circulation* 2006; **114**: 1581–1590.
42. Schmacht L, Traber J, Grieben U, Utz W, Dieringer MA, Kellman P, Blaszczyk E, von Knobelsdorff-Brenkenhoff F, Spuler S, Schulz-Menger J. Cardiac involvement in myotonic dystrophy type 2 patients with preserved ejection fraction: detection by cardiovascular magnetic resonance. *Circ Cardiovasc Imaging* 2016; **9**.
43. Blaszczyk E, Grieben U, von Knobelsdorff-Brenkenhoff F, Kellman P, Schmacht L, Funk S, Spuler S, Schulz-Menger J. Subclinical myocardial injury in patients with Facioscapulohumeral muscular dystrophy 1 and preserved ejection fraction—assessment by cardiovascular magnetic resonance. *J Cardiovasc Magn Reson* 2019; **21**: 25.
44. Mavrogeni S, Papavasiliou A, Skouteli E, Magoutas A, Dangas G. Cardiovascular magnetic resonance imaging evaluation of two families with Becker muscular dystrophy. *NMD* 2010; **20**: 717–719.
45. Yilmaz A, Gdynia HJ, Baccouche H, Mahrholdt H, Meinhardt G, Basso C, Thiene G, Sperfeld AD, Ludolph AC, Sechtem U. Cardiac involvement in patients with Becker muscular dystrophy: new diagnostic and pathophysiological insights by a CMR approach. *J Cardiovasc Magn Reson* 2008; **10**: 50.
46. Kanagala P, Cheng ASH, Singh A, Khan JN, Gulsin GS, Patel P, Gupta P, Arnold JR, Squire IB, Ng LL, McCann GP. Relationship between focal and diffuse fibrosis assessed by CMR and clinical outcomes in heart failure with preserved ejection fraction. *J Am Coll Cardiol Img* 2019; **12**: 2291–2301.